

β -Cell Obligation in α -Cell Glucagon Response to Low Glucose

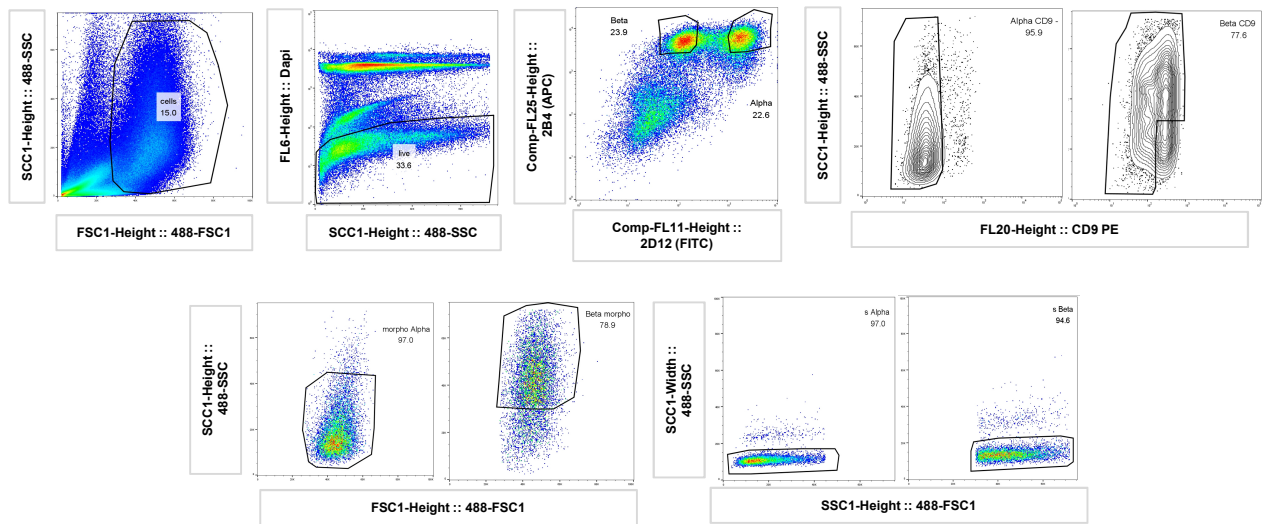
By

Eva Bru-Tari*#, Marta Perez-Frances*, Fabrizio Thorel and Pedro L. Herrera#

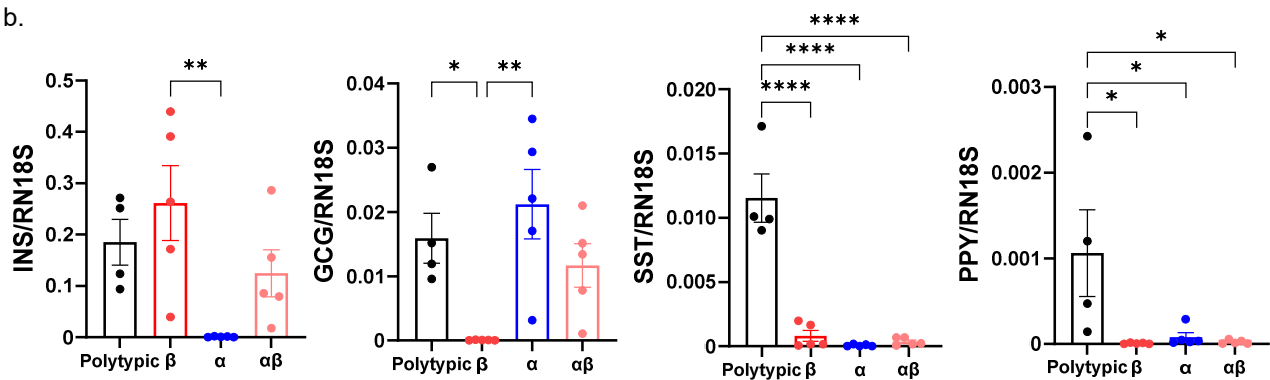
Dept. of Genetic Medicine & Development, iGE3 and Centre facultaire du diabète,
Faculty of Medicine, University of Geneva, 1206 Geneva, Switzerland

Supplemental Figure 1

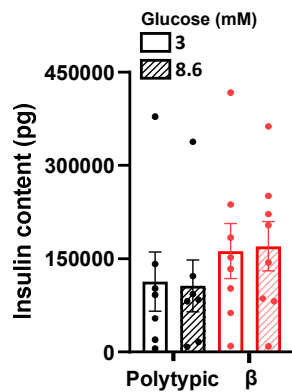
a.



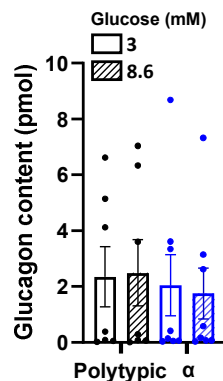
b.



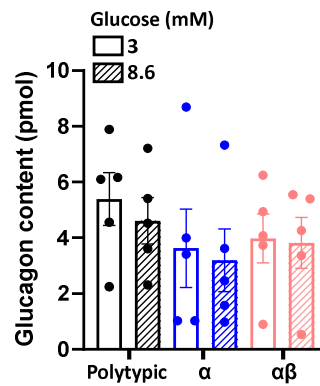
c.



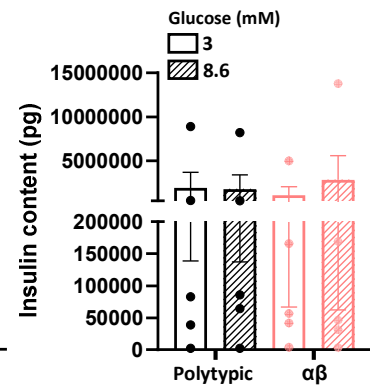
d.



e.

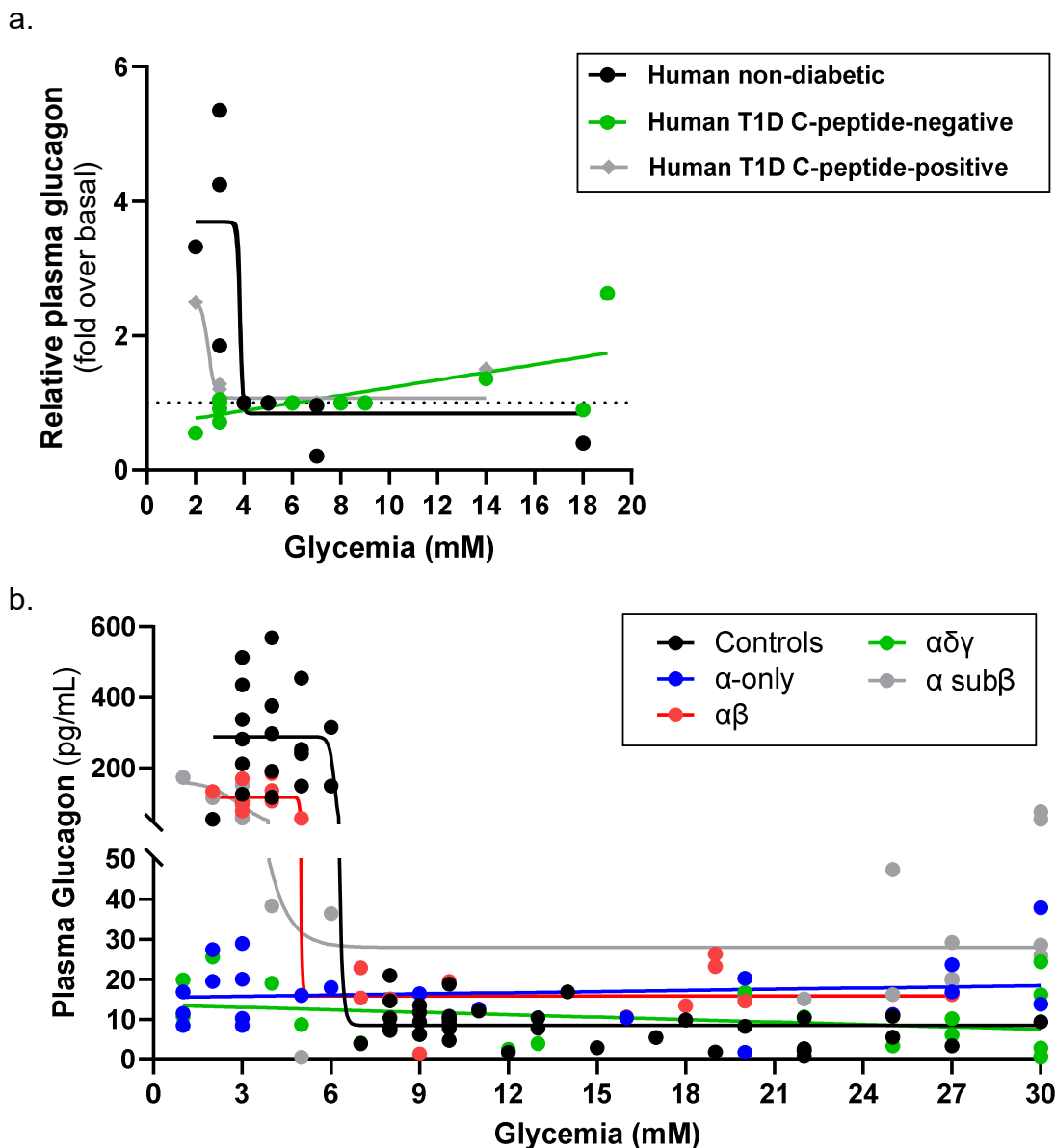


f.



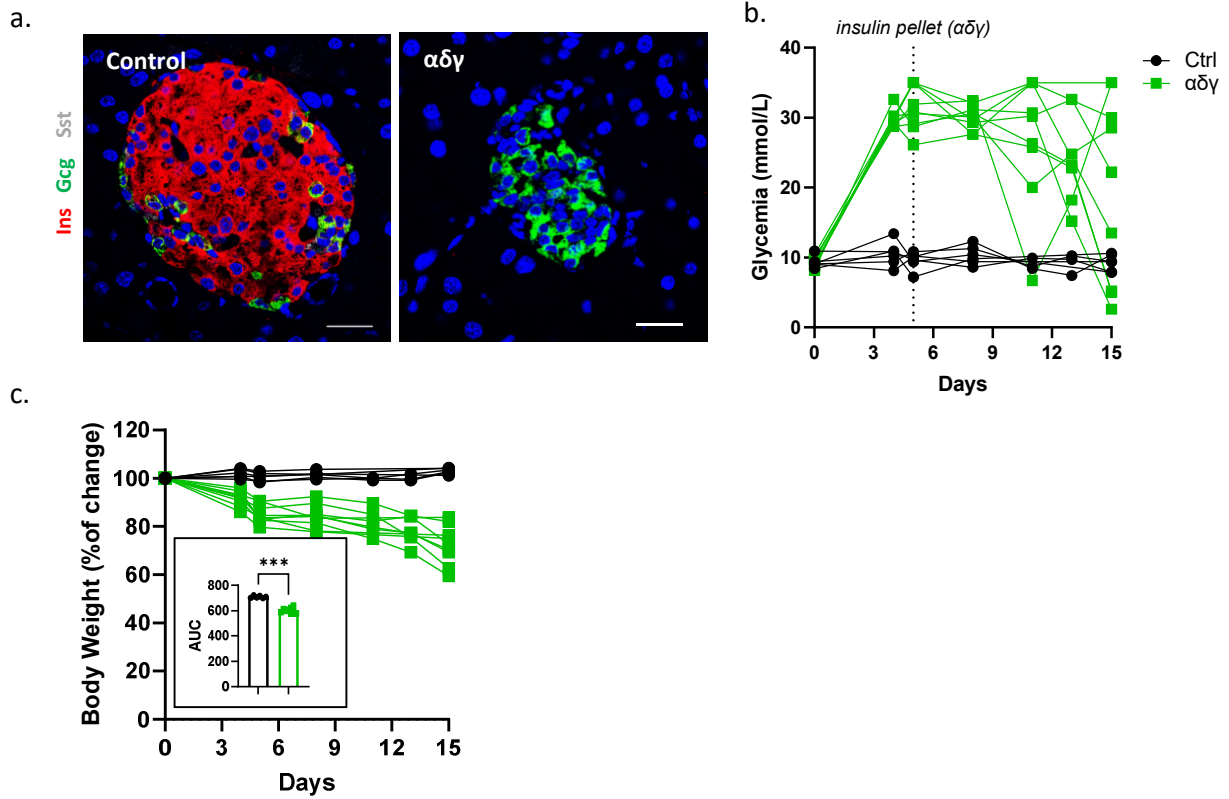
Supplemental Figure 1. Characterization of FACS-purified human α - and β -cell populations and pseudoislet hormone content. **a.** FACS strategy used to purify human β - and α -cells. Representative plots show cells labelled with the pan-endocrine marker H1C1-2B4, the non- β -cell endocrine marker H1C3-2D12 and the marker CD9, allowing high purity isolation of α - and β -cells. **b.** RT-qPCR analysis of *INS*, *GCG*, *SST* and *PPY* expression on polytypic, α -pseudoislets and $\alpha\beta$ -pseudoislets. Data are normalized to the housekeeping gene *RN18S*. N=4-5 donors. **c.** Total insulin content of polytypic (black) and β -pseudoislets (red) after stimulation at 3 mM and 8.6 mM glucose (from figure 1d). **d.** Total glucagon content of polytypic (black) and α -pseudoislets (blue) after stimulation at 3 mM and 8.6 mM glucose (from figure 1f). **e.** Total glucagon content of polytypic, α - and $\alpha\beta$ -pseudoislets (from figure 2d). **f.** Total insulin content of polytypic and $\alpha\beta$ -pseudoislets (from figure 2d). All data are shown as mean \pm sem. One-way ANOVA with Turkey's multiple comparison test (b, c, d). Two-way ANOVA with Turkey's multiple comparison test (e, f). Raw data are provided as Source data Supplemental Figure 1.

Supplemental Figure 2



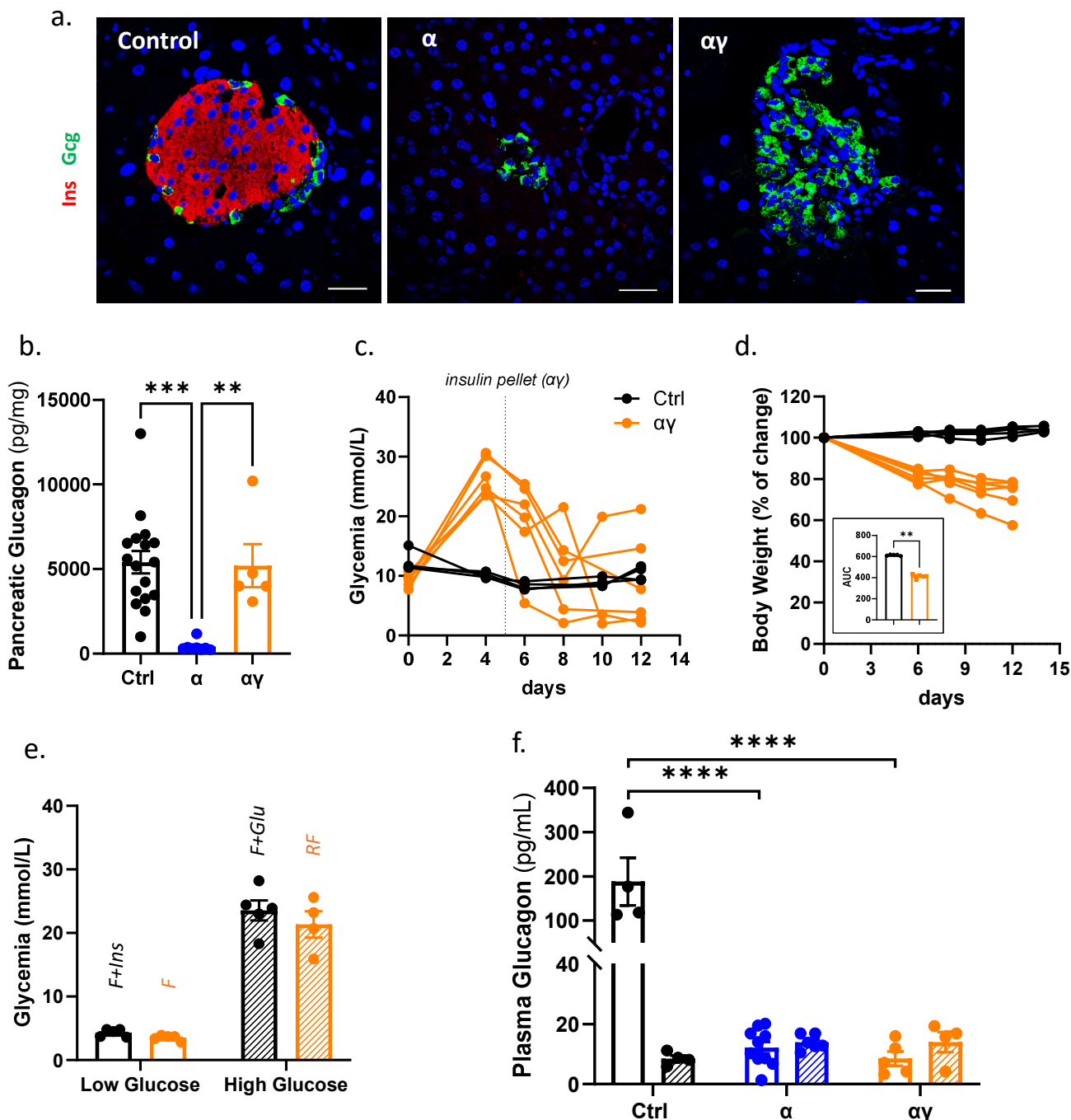
Supplemental Figure 2. Integrated human and mouse analyses correlate the persistence of residual β -cells with preserved counterregulatory glucagon responses. **a.** Human meta-analysis. Data were compiled from 9 published studies reporting concurrent plasma glucagon and glucose measurements in non-diabetic and T1D subjects. T1D participants stratified by residual β -cell function (C-peptide-positive, grey; C-peptide negative, green). Values were converted to common units and normalized to each study's basal glucagon level to yield fold-change responses across the glycemic range. Each point represents a study-level mean. Non-diabetic subjects and T1D participants with detectable circulating C-peptide exhibited glucose-dependent levels of glucagon and were therefore analyzed using a four-parameter logistic model (non-diabetic, $R^2 = 0.76$; T1D C-peptide-positive, $R^2 = 0.865$). In contrast, T1D C-peptide-negative glucagon response lacked a sigmoidal relationship and displayed a significant linear slope ($R^2 = 0.459$; $P = 0.0039$ vs zero slope). Model fits were compared by extra-sum-of-squares F-test, and goodness-of-fit was evaluated by R^2 . Dashed line indicates fold over basal = 1. **b.** Mouse data generated for this study. Plasma glucagon levels (pg/ml) were measured across a glucose range of 0-30 mM in control (Ctrl, black, $n=20$), " α " (blue, $n=22$), " $\alpha\beta$ " (green, $n=9$), " $\alpha\delta\gamma$ " (red, $n=9$) and " α sub β " mice (grey, $n=12$). Data was analyzed using a four-parameter logistic model (4PL, control: $R^2 = 0.72$; " $\alpha\beta$ ": $R^2 = 0.84$; " α sub β ": $R^2 = 0.74$). " α " and " $\alpha\delta\gamma$ " displayed a linear slope (" α ": $R^2 = 0.02$; " $\alpha\delta\gamma$ ": $R^2 = 0.08$). Model fits were compared by extra-sum-of-squares F-test, and goodness-of-fit was evaluated by R^2 . Raw data provided as Source data Supplemental Figure 2.

Supplemental Figure 3



Supplemental Figure 3. Selective and efficient ablation of target cell populations in $\alpha\delta\gamma$ mice. **a.** Immunofluorescence staining of control and “ $\alpha\delta\gamma$ ” mice. INS: red; GCG: green; SST: gray. Scale bar: 20 μ m. **b.** Glycemia over 15 days after first DT injection in control (Ctrl, black, n=6) and “ $\alpha\delta\gamma$ ” (green, n=9) mice. **c.** Percentage of body weight change in control (black, n=6) and “ $\alpha\delta\gamma$ ” (green, n=9) mice. Inset: Area under the curve (AUC) of body weight change. Two-tailed Mann-Whitney test. All data are shown as mean \pm sem. Raw data are provided as Source data Supplementary Figure 3.

Supplemental Figure 4



Supplemental Figure 4. $\alpha\gamma$ mice maintain normal pancreatic glucagon content but display impaired counterregulatory glucagon secretion.

a. Immunofluorescence staining of control, " α " and " $\alpha\gamma$ " mice. INS: red; GCG: green; SST: gray. Scale bar: 20 μ m. **b.** Pancreatic glucagon content (pg/mg) in control (black, n=17), " α " (blue, n=8) and " $\alpha\gamma$ " (orange, n=5) mice. **c.** Glycemia over 15 days after first DT injection in control (Ctrl, black, n=4) and " $\alpha\gamma$ " (orange, n=6) mice. **d.** Percentage of body weight change in control (black, n=5) and " $\alpha\gamma$ " (orange, n=6) mice. Inset: Area under the curve (AUC) of body weight change. **e.** Glycemia of control (black, n=5) and " $\alpha\gamma$ " (orange, n=4) mice before blood collection at low (dashed bar) and high (fill bar) glucose levels. Mice were fasted (F) or random fed (RF) and injected with intra-peritoneal insulin (Ins) or glucose (Glu). **f.** Plasma glucagon (pg/ml) in control (black, n=4), " α " (blue, Low G: n=10; High G: n=6) and " $\alpha\gamma$ " (orange, Low G: n=5; High G: n=4) at low (dashed bar) and high (continuous bar) glucose levels. Data from f: " α " was used as reference from figure 3f. Statistical comparisons between groups in at each glucose condition were performed using one-way ANOVA with Tukey's post-hoc test (*). Comparisons between low vs high glucose within each group were performed using two-tailed Mann Whitney test (#). One-way ANOVA with multiple comparisons test (e); two-tailed Mann-Whitney test (b, d). All data are shown as mean \pm sem. Raw data are provided as Source data Supplementary Figure 4.